

Dynamic Resonant Frequency Bands of Suspension System of Vehicles with Varying Speeds Based on Time-Frequency Spectrum

ZHANG Buyun^{1*}, ZENG Falin^{1, 2}, TAN Chin-An²

1. Automotive Engineering Research Institute, Jiangsu University, Zhenjiang 212013, P.R. China;

2. Department of Mechanical Engineering, Wayne State University, Detroit 48202, USA

(Received 12 October 2019; revised 1 April 2020; accepted 1 February 2021)

Abstract: The dynamic responses of suspension system of a vehicle travelling at varying speeds are generally non-stationary random processes, and the non-stationary random analysis has become an important and complex problem in vehicle ride dynamics in the past few years. This paper proposes a new concept, called dynamic frequency domain (DFD), based on the fact that the human body holds different sensitivities to vibrations at different frequencies, and applies this concept to the dynamic assessment on non-stationary vehicles. The study mainly includes two parts, the first is the input numerical calculation of the front and the rear wheels, and the second is the dynamical response analysis of suspension system subjected to non-stationary random excitations. Precise time integration method is used to obtain the vertical acceleration of suspension barycenter and the pitching angular acceleration, both root mean square (RMS) values of which are illustrated in different accelerating cases. The results show that RMS values of non-stationary random excitations are functions of time and increase as the speed increases at the same time. The DFD of vertical acceleration is finally analyzed using time-frequency analysis technique, and the conclusion is obviously that the DFD has a trend to the low frequency region, which would be significant reference for active suspension design under complex driving conditions.

Key words: non-stationary random process; suspension system; vehicle modeling; dynamical frequency domain (DFD); ride comfort

CLC number: O324

Document code: A

Article ID: 1005-1120(2021)02-0333-11

0 Introduction

Road excitations to a vehicle may be non-stationary random processes as a result of the vehicle's varying speeds. It has been shown that non-stationary characteristics can have significant effects on vehicle ride comfort, handling performance, and safety^[1-3]. With vehicle technologies moving towards intellectualization, electrification and integration, the detrimental consequences due to non-stationary driving can be profound. For instance, several studies have reported that such non-stationary vibration may shorten the power battery life of new energy ve-

hicles^[4-5], which is a research hotspot in automotive industry, bringing great challenges to ensure the stability and reliability of the complex electromechanical hydraulic coupling systems in these vehicles^[6-7]. Therefore, understanding the non-stationary vibration characteristics is essential for the analysis and development of control systems to improve the quality of vehicle driving. Traditional suspension control focused on the entire frequency range or some finite fixed frequency range of interest^[8]. However, the frequency ranges of interest for suspension control are often time-varying since the vibration responses of a vehicle body subjected to non-stationary ran-

*Corresponding author, E-mail address: zhangby@ujs.edu.cn.

How to cite this article: ZHANG Buyun, ZENG Falin, TAN Chin-An. Dynamic resonant frequency bands of suspension system of vehicles with varying speeds based on time-frequency spectrum [J]. Transactions of Nanjing University of Aeronautics and Astronautics, 2021, 38(2): 333-343.

<http://dx.doi.org/10.16356/j.1005-1120.2021.02.014>

dom excitations are non-stationary processes. Moreover, the resonant frequency bands will change as well due to the varying speeds.

The dynamics of vehicles subjected to stationary road excitations is well understood^[9], and research results have been extensively applied to the automotive industry. However, several key obstacles remain for the non-stationary problem. The first step that is essential for studying the non-stationary random vibration problem is to obtain accurate road information. The frequency domain model is one of the most effective road excitation models and has been employed extensively in vehicle dynamics analysis due to the well-known theories. Parkhilovskii^[10] and Dodds and Robson^[11] were among the early researchers to put forth frequency domain road models. They developed statistic characteristics analyses to profile the road roughness for different kinds of road surfaces, with excitations to the wheels modeled as ergodic stationary random processes. Such models are generally inadequate because more complex dynamic analysis of vehicle structural systems is required in modern automotive technologies. Time domain models are more suitable to describe the road profile and have widely been adopted for several decades^[12-17]. However, the amount of computation time was huge. To overcome the obstacle, Marzbanrada and Ahmadib^[18] proposed a linear filtering white noise model which resulted in a much less computation time and faster speed. Zhang et al.^[19] used a novel method called Cholesky decomposition filtering white noise to generate new random signals. However, the process was too complex and the simulation precision was not sufficient in practice.

From aforementioned research, it is clear that neither the frequency nor the time domain model can satisfactorily analyse the non-stationary random processes. Recent research efforts have focused on developing suitable models and analysis methods for vehicles subjected to non-stationary random excitations^[20-22]. Lei et al.^[23] modeled and simulated the power spectral density (PSD) of non-stationary random road excitations as a Wiener process. Zhang et al.^[24] used the equivalent covariance method to es-

tablish a non-stationary random input model for a single wheel and resolved the correlation between the front and the rear wheels with a variable time lag. However, the derivative process employed in these two papers was too tedious to be applied efficiently to a vehicle system analysis. In Refs. [25-26], a non-geometric approach was applied to define the spectral characteristics of non-stationary processes in the response analysis of a simple oscillator, with only the first three non-stationary spectral characteristics of the response being considered. Marbato and Conte^[27] pointed out that the approach to describe non-stationary random processes was not unique, and extended definitions of spectral characteristics of non-stationary processes from real-to complex-valued functions to more adequately model the processes.

In summary, many studies have been devoted to understand the responses of suspension systems subjected to road excitations and most of these works were based on the assumption of stationary ergodic random vibration processes in which frequency domain analysis is sufficient. However, for non-stationary random vibration analysis, statistical characteristics must be examined in both the time and frequency domains. In this paper, the response of a half-car suspension system to non-stationary road excitations was examined for different acceleration cases. Linear time variable method was applied to transfer the road stationary random process in the spatial domain to the non-stationary inputs in the time domain. The vertical acceleration of suspension barycenter and the pitch angular acceleration were obtained by the precise time integration method (PTIM). The response vibration level with indicator as root mean square (RMS) values varying with time was illustrated and finally the dynamic frequency domain (DFD) characteristics were performed using time-frequency analysis method.

1 General Description of Responses of Vehicle Suspension System to Road Excitation

In this paper, we consider the vehicle suspen-

sion system as a linear, multi-degree-of-freedom (MDOF) vibration system. Since the system is excited by non-stationary random excitations, the responses are also non-stationary processes. In order to describe the characteristics of the non-stationary responses more adequately, it is necessary to introduce additional concepts in the time-frequency domain.

Road surface irregularity is the main excitation source that causes the suspension system to vibrate. The road profiles are stationary random processes and are usually described by the PSD in spatial frequency domain. In general, the frequency band of road surface irregularity does not exceed 10 m^{-1} , as shown in Fig.1. From Fig.1, we can see that the road surface can be divided into eight classes, represented by letters from A to H, with H class representing the worst case of road surface

(i.e., this road surface is the roughest). For linear MODF suspension systems, the resonant frequencies are usually in the range of 1—10 Hz. For a vehicle traveling at a constant speed, the response PSD of the suspension system is the product of the PSD of road surface irregularity and the square of Fourier transform of frequency response function (FRF) of the vibration system. In this case, the resonant frequency band of responses is comparatively stable. However, when the vehicle travels at varying speeds, the excitation spectrum will be represented in both time and frequency domains. The responses are non-stationary signals and hence the peak band, called the dynamic frequency domain in this paper, is also varying, as shown in Fig.1. Vehicle ride comfort and handling performances can be improved efficiently by attenuating the vertical vibration.

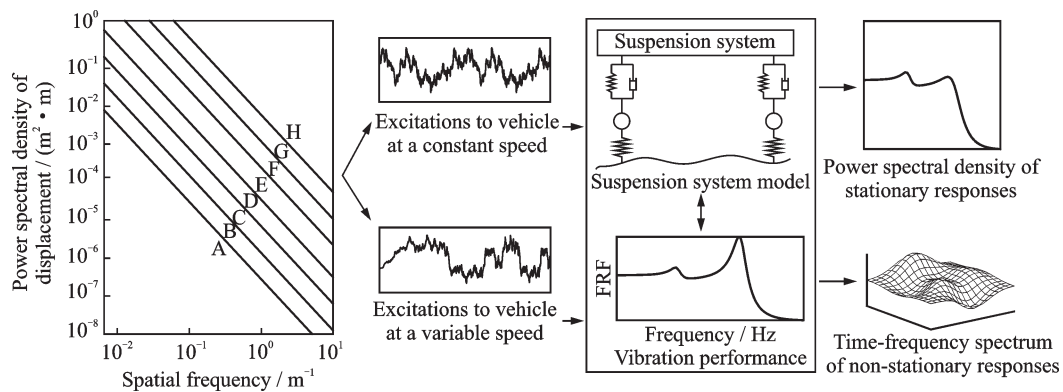


Fig.1 Vibration responses of vehicle suspension system subjected to different excitations including both stationary and non-stationary random processes

2 Modeling of Vehicle Suspension and Road Excitation

A half vehicle model is employed to describe the ride performance. It is easier to compute than a full car model, and also capable of modeling the pitch angular acceleration and the coherence characteristics between the front and the rear wheels. When a vehicle travels at varying speeds, its vertical acceleration, suspension displacement, and dynamic tire loads are much more complex than those in the constant speed case. The vehicle model is illustrated in Fig.2. Table 1 shows the values

of the parameters for the system considered in this study.

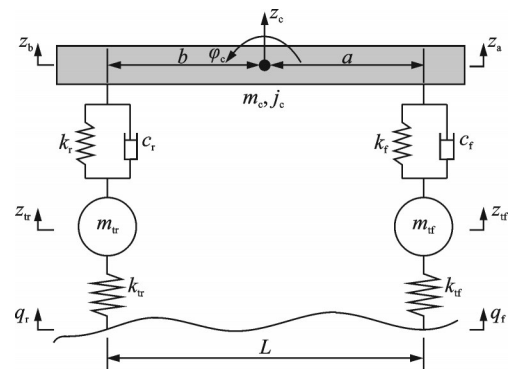


Fig.2 Half vehicle model with 4-DOF

Table 1 Parameters and values of suspension system

Parameter	Symbol	Value
Unsprung mass of the front wheel /kg	m_{tf}	39.5
Unsprung mass of the rear wheel / kg	m_{tr}	44.4
Body mass of half vehicle /kg	m_c	680
Pitching rotational inertia / (kg·m ²)	J_c	1 120
Stiffness of the front wheel / (N·m ⁻¹)	k_{tf}	106 420
Stiffness of the rear wheel / (N·m ⁻¹)	k_{tr}	115 270
Spring stiffness of the front suspension / (N·m ⁻¹)	k_f	10 000
Spring stiffness of the rear suspension / (N·m ⁻¹)	k_r	9 500
Damping of the front suspension / (N·(m·s ⁻¹) ⁻¹)	c_f	1 050
Damping of the rear suspension / (N·(m·s ⁻¹) ⁻¹)	c_r	1 110
Distance from barycenter to the front suspension / m	a	1.3
Distance from barycenter to the rear suspension / m	b	1.5
Wheel base / m	L	2.8

2.1 Road surface excitation

The loads at the front and the rear wheels generated by road surface excitations are the same in the spatial frequency domain, but there is a certain time difference in time domain.

The road surface irregularity is a stationary random process but the excitation to each wheel is a non-stationary random process when the vehicle speed is varying. It represents a linear time varying system with a stationary random process as input and the output is a non-stationary random process. Assume that the road surface is of class C and the irregularity coefficient is

$$G_q(n_0) = 2.56 \times 10^{-4} \text{ m}^2/\text{m}^{-1} \quad (1)$$

where $n_0 = 0.1 \text{ m}^{-1}$ is a reference spatial frequency. The front wheel input $q_f(t)$ can be obtained by employing a linear relationship between the input/output of a vibratory system as

$$\dot{q}_f(t) + v(t)\Omega_c q_f(t) = A(t)W(t) \quad (2)$$

where $v(t)$ is the vehicle speed expressed as a func-

tion of time t . For a vehicle with constant acceleration a , the speed is $v(t) = v_0 + at$, $\Omega_c = 2\pi n_c$, $n_c = 0.01 \text{ m}^{-1}$ is the cutoff spatial frequency. $A(t) = n_0 \sqrt{2\pi G_q(n_0) v(t)}$ is the non-stationary modulation function and $W(t)$ the stationary process.

2.1.1 Input to the front wheel

In order to get the front wheel input $q_f(t)$, PTIM is adopted because of its high computation precision and faster efficiency^[28]. We can rewrite Eq.(2) in the standard form of PTIM as

$$\dot{q}_f(t) = Hq_f(t) + R \quad (3)$$

where $H = -v(t)\Omega_c$ and $R = A(t)W(t)$. The numerical solution to Eq.(3) includes two parts: The homogeneous and particular solutions. The homogeneous solution may be written in the form of

$$q_{f,g}(t_i) = e^{Ht_i} q_f(0) = e^{H \cdot i\Delta t} q_f(0) \quad (4)$$

where $q_f(0)$ is the initial condition. If time interval Δt was determined, the exponential matrix $e^{H \cdot i\Delta t}$ in the equation may be easily obtained^[29-30]. Next, we need to calculate the particular solution

$$q_{f,s}(t_i) = \int_0^{t_i} e^{H(t_i - \xi)} R(\xi) d\xi \quad (5)$$

The above integral can be evaluated using the 3-point Gauss-Legendre integral formula given by

$$\int_a^b f(x) dx = \frac{b-a}{2} \int_{-1}^1 f\left(\frac{b-a}{2}t + \frac{b+a}{2}\right) dt = \frac{b-a}{2} \sum_{i=0}^2 X_i f\left(\frac{b-a}{2}\xi_i + \frac{b+a}{2}\right) + o(f) \quad (6)$$

where ξ_i is called the Gauss integration point, X_i the integration coefficient, and $o(f)$ the residual item of error. Suppose that

$$\xi = i\Delta t + \frac{\Delta t}{2}(1 + \xi_i) \quad (7)$$

Substituting Eqs.(6-7) into Eq.(5) gives

$$q_{f,s}(t_{i+1}) = \frac{\Delta t}{2} \sum_{i=0}^2 X_i e^{\frac{\Delta t}{2}(1 - \xi_i)} R\left[t_i + \frac{\Delta t}{2}(1 + \xi_i)\right] + o(\Delta t^6) \quad (8)$$

2.1.2 Input to the rear wheel

As mentioned above, the time lag τ between the two wheel inputs is constant when the driving speed does not vary, but τ is a function time when the vehicle speed varies. The time lag τ can be obtained by dividing the wheel base L by the speed v as

$$\tau = L/v \tag{9}$$

Since the road surface irregularity is described in the spatial domain while the excitation to the wheels is expressed in time domain, the excitation at time t can be expressed by the road roughness at $s(t)$ ^[31]. Under the premise that the front input was obtained, the rear input could be expressed by

$$q_r(t) = q_f(t - \tau) = q[s(t) - L] \tag{10}$$

This equation cannot be transformed by FFT but can be expanded through Taylor series expansion. By omitting the higher order items, we can get (omitting the second order item)

$$q_r(t) = q_f[s(t)] - \frac{L}{v} \frac{dq_f(t)}{dt} + \frac{1}{2} \left(\frac{L}{v}\right)^2 \left(\frac{d^2 q_f(t)}{dt^2} - \frac{a}{v} \frac{dq_f(t)}{dt}\right) + \dots = q_f[s(t)] - \frac{L}{v} \frac{dq_f(t)}{dt} \tag{11}$$

Taking the derivative of both sides of Eq.(11), we obtain

$$\dot{q}_r(t) = \dot{q}_f(t) + \frac{La}{v^2} \dot{q}_f(t) - \left(\frac{L}{v}\right) \ddot{q}_f(t) \tag{12}$$

Given

$$\ddot{q}_r(t) = 2\left(\frac{v}{L}\right)^2 \left[q_r(t) - q_f(t) + \left(\frac{L}{v}\right) \dot{q}_f(t) + \frac{1}{2} \left(\frac{L}{v}\right)^2 \frac{a}{v} q_f(t) \right] \tag{13}$$

we can get the rear wheel input with the front wheel input and instantaneous speed of

$$\dot{q}_r(t) = -\left(\frac{2v}{L}\right) q_r(t) - \dot{q}_f(t) + \left(\frac{2v}{L}\right) q_f(t) \tag{14}$$

2.1.3 Validation of PTIM simulation on a cantilever beam

Compared with other methods, the responses of a cantilever beam subjected to different types of excitation are analyzed to verify the reliability and accuracy of PTIM. The geometry and input-output points setting of the cantilever beam are shown in Fig.3. The length of the beam is 1 000 mm, and

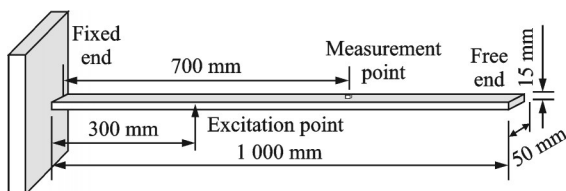


Fig.3 Geometrical parameters of cantilever beam model

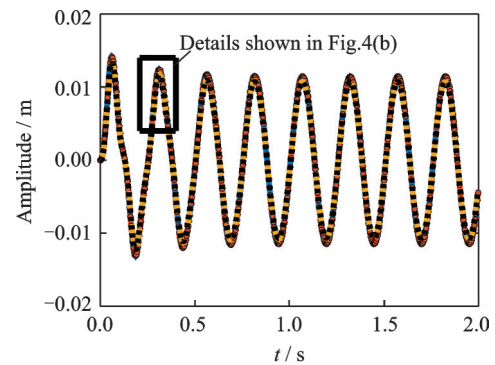
the excitation point and measurement point are set at 300 mm and 700 mm from the fixed end, respectively. On one hand, the analytical responses at the measurement point subjected to the excitations including sinusoidal or random signals can be obtained exactly through vibration theory. On the other hand, the responses can also be calculated by finite element analysis method. In this section, several methods such as Newmark, Wilson- θ and NPIM are selected to compare with the analysis results.

To avoid the resonance case, it is better to calculate the natural frequencies of the cantilever beam first, as shown in Table 2. The values are exactly according to analytical calculation.

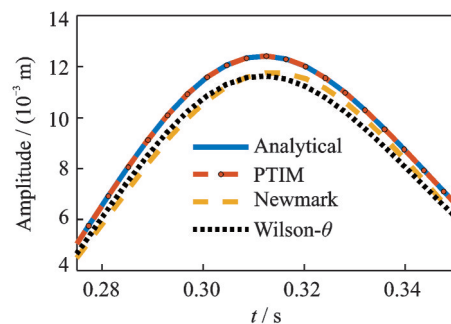
Table 2 The first five natural frequencies of the beam

Order	1st	2nd	3rd	4th	5th
Frequency / Hz	12.23	76.65	214.62	420.59	695.34

We use two different sinusoidal signals at 4 Hz and 23.9 Hz to excite the beam, and the responses are shown in Fig.4 and Fig.5, respectively. From the figures we can conclude that PTIM has an accurate calculation with the analytical results. No mat-

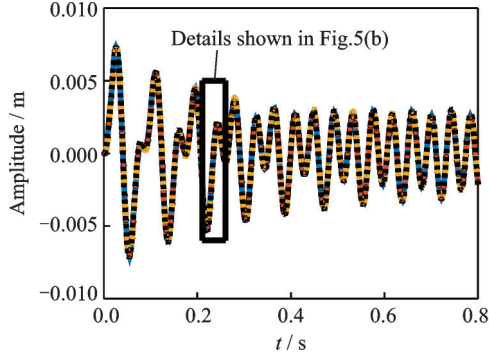


(a) Responses of beam from start to 2 s

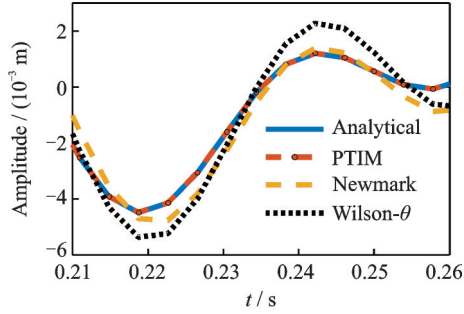


(b) Details between 0.275 s and 0.345 s

Fig.4 Responses at 4 Hz excitation and detail illustration



(a) Responses of beam from start to 0.8 s



(b) Details between 0.21 s and 0.26 s

Fig.5 Responses at 23.9 Hz excitation and detail illustration

ter in low-frequency or high-frequency domain, it has higher accuracy than the other two methods, which can meet the requirements of input and output calculation in vehicle dynamics.

2.2 Governing equations of motion

According to dynamic law, the equation of motion of the vehicle system shown in Fig.2 is

$$H = \begin{bmatrix} 0 & 1 & 0 & 0 & 0 & 0 & 0 & 0 \\ -\frac{k_f + k_r}{m_c} & -\frac{c_f + c_r}{m_c} & \frac{bk_r - ak_f}{m_c} & \frac{bc_r - ac_f}{m_c} & \frac{k_f}{m_c} & \frac{c_f}{m_c} & \frac{k_r}{m_c} & \frac{c_r}{m_c} \\ 0 & 0 & 0 & 1 & 0 & 0 & 0 & 0 \\ \frac{bk_r - ak_f}{J_c} & \frac{bc_r - ac_f}{J_c} & -\frac{a^2 k_f + b^2 k_r}{J_c} & -\frac{a^2 c_f + b^2 c_r}{J_c} & \frac{ak_f}{J_c} & \frac{ac_f}{J_c} & -\frac{bk_r}{J_c} & -\frac{bc_r}{J_c} \\ 0 & 0 & 0 & 0 & 0 & 1 & 0 & 0 \\ \frac{k_f}{m_{tf}} & \frac{c_f}{m_{tf}} & \frac{ak_f}{m_{tf}} & \frac{ac_f}{m_{tf}} & -\frac{k_f + k_{tf}}{m_{tf}} & -\frac{c_f}{m_{tf}} & 0 & 0 \\ 0 & 0 & 0 & 0 & 0 & 0 & 0 & 1 \\ \frac{k_r}{m_{tr}} & \frac{c_r}{m_{tr}} & -\frac{bk_r}{m_{tr}} & -\frac{bc_r}{m_{tr}} & 0 & 0 & -\frac{k_r + k_{tr}}{m_{tr}} & -\frac{c_r}{m_{tr}} \end{bmatrix}$$

$$C = \begin{bmatrix} 0 & 1 & 0 & 0 & 0 & 0 & 0 & 0 \\ 0 & 0 & 0 & 1 & 0 & 0 & 0 & 0 \\ 0 & 0 & 0 & 0 & 0 & 0 & 0 & 0 \\ 0 & 0 & 0 & 0 & 0 & 0 & 0 & 0 \end{bmatrix}, D = \begin{bmatrix} 0 & 1 & 0 & 0 & 0 & 0 & 0 & 0 \\ 0 & 0 & 0 & 1 & 0 & 0 & 0 & 0 \\ 1 & 0 & a & 0 & -1 & 0 & 0 & 0 \\ 1 & 0 & -b & 0 & 0 & 0 & -1 & 0 \end{bmatrix}$$

$$\begin{cases} m_c \ddot{z}_c + c_f(\dot{z}_a - \dot{z}_{tf}) + k_f(z_a - z_{tf}) + \\ c_r(\dot{z}_b - \dot{z}_{tr}) + k_r(z_b - z_{tr}) = 0 \\ J_c \ddot{\varphi}_c + a[c_f(\dot{z}_a - \dot{z}_{tf}) + k_f(z_a - z_{tf})] - \\ b[c_r(\dot{z}_b - \dot{z}_{tr}) + k_r(z_b - z_{tr})] = 0 \\ m_{tf} \ddot{z}_{tf} + c_f(\dot{z}_{tf} - \dot{z}_a) + k_f(z_{tf} - z_a) + \\ k_{tf}(z_{tf} - q_f) = 0 \\ m_{tr} \ddot{z}_{tr} + c_r(\dot{z}_{tr} - \dot{z}_b) + k_r(z_{tr} - z_b) + \\ k_{tr}(z_{tr} - q_r) = 0 \end{cases} \quad (15)$$

The items' meanings in Eq.(15) are shown in Table 1. The relationships among z_a , z_b , z_c , and φ_c are

$$\begin{cases} z_b = z_c - b \tan \varphi_c \approx z_c - b \varphi_c \\ \dot{z}_b = \dot{z}_c - b(\sec^2 \varphi_c) \dot{\varphi}_c \approx \dot{z}_c - b \dot{\varphi}_c \\ z_a = z_c + a \tan \varphi_c \approx z_c + a \varphi_c \\ \dot{z}_a = \dot{z}_c + a(\sec^2 \varphi_c) \dot{\varphi}_c \approx \dot{z}_c + a \dot{\varphi}_c \end{cases} \quad (16)$$

Next, the state vector is set as

$$\mathbf{v} = [z_c \quad \dot{z}_c \quad \varphi_c \quad \dot{\varphi}_c \quad z_{tf} \quad \dot{z}_{tf} \quad z_{tr} \quad \dot{z}_{tr}]^T \quad (17)$$

and the output vector is

$$\mathbf{y} = [\ddot{z}_c \quad \ddot{\varphi}_c \quad z_a - z_{tf} \quad z_b - z_{tr}]^T \quad (18)$$

PTIM is still to be used and the state equations may be written as

$$\begin{cases} \dot{\mathbf{v}} = H\mathbf{v} + \mathbf{r} \\ \mathbf{y} = C\dot{\mathbf{v}} + D\mathbf{v} \end{cases} \quad (19)$$

where the terms in the above equations are defined as

$$\mathbf{r} = \begin{bmatrix} 0 & 0 & 0 & 0 & 0 & \frac{k_{tf}}{m_{tf}} q_f & 0 & \frac{k_{tr}}{m_{tr}} q_r \end{bmatrix}^T$$

3 Simulation and Discussions

The suspension system responses of vehicle traveling at variable speeds may be calculated by the following steps.

Step 1 Determine the excitation signals of the front and the rear wheels according to running conditions, road surface irregularity, and the structural parameters of vehicle.

Step 2 Establish the half vehicle model and obtain the vibration performance.

Step 3 Use the numerical integration approach and PTIM to simulate the interest responses of suspension, mainly including the vertical acceleration of suspension barycenter and the proposed pitching angular acceleration.

Step 4 Analyse the response by time-frequency method, and focus on the DFD's varying trend with speeds, obtaining the DFD characteristics of suspension system under non-stationary random excitation.

The PSD of C class road surface is shown in Fig.6(a), and the altitude data in spatial amplitude domain may be obtained using trigonometric series method as shown in Fig.6(b).

In this paper, the vehicle starts moving at initial state of rest with an acceleration of 2 m/s^2 . With the traveling time of 14 s, the traveling distance is 196 m. The excitation signals of the front and the

rear wheels in time domain are exhibited in Fig.7. Fig.7 shows that there is a time lag of the two inputs, and the lag is a variable that has an absolute relationship with the vehicle velocity.

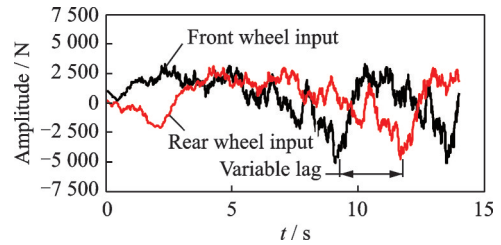
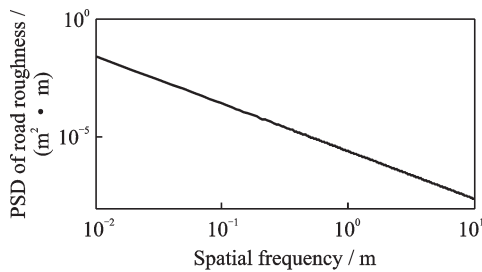
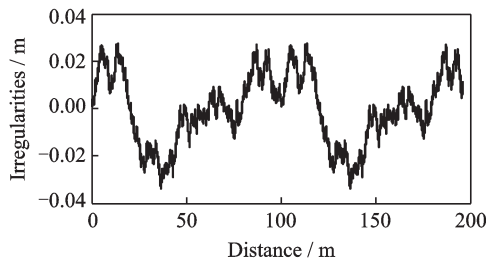


Fig.7 Excitation of the front and the rear wheels in time domain

Fig.8(a) shows the vertical acceleration of suspension barycenter, and Fig.8(b) represents the pitching angular acceleration. X axis represents the simulation time. On one hand, we can draw the conclusion from the figures that the level of vibration increases with the increased speed, especially after 8 s. When the speed is 57.6 km/h, the amplitude increases obviously. On the other hand, if the vehicle rides at the varying speeds, no matter the vertical acceleration of suspension barycenter nor the pitching angular acceleration would be stationary process as illustrated distinctly in Fig.8(c) and Fig.8(d). The comparison between the two cases implies that the vibration response level of vehicles increases continuously due to the non-stationary random excitation, so that some new control algorithms should

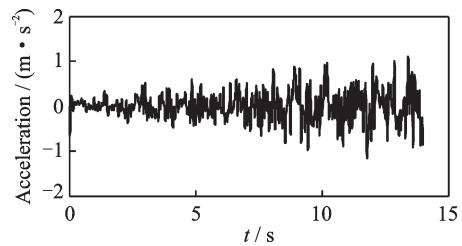


(a) Spatial frequency domain

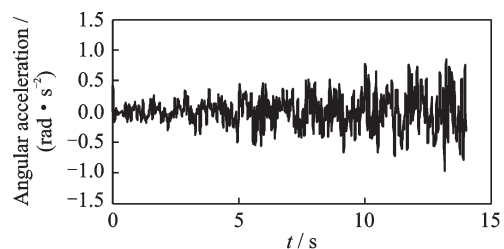


(b) Spatial amplitude domain

Fig.6 Illustration of road surface irregularity



(a) Vertical acceleration of suspension barycenter in accelerating case



(b) Pitching angular acceleration in accelerating case

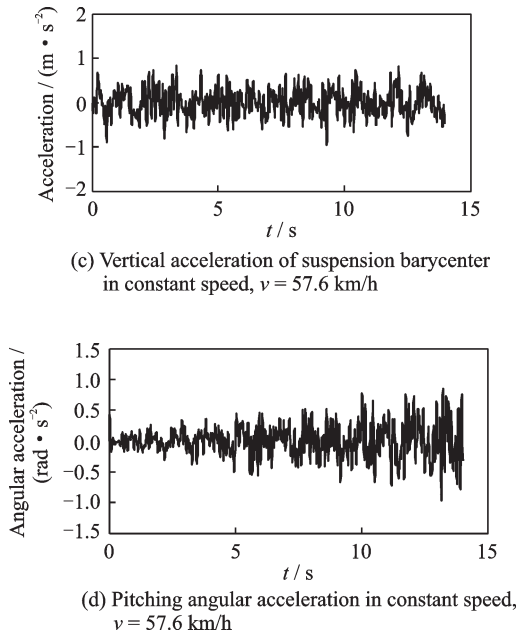


Fig.8 Responses of suspension systems

be considered to deal with this situation. This would be the follow-up work of this paper.

In order to compare the responses under different traveling conditions, three different acceleration cases are used for simulation and the RMS of responses are shown in Fig.9. The results show that both the vertical acceleration of suspension barycenter and pitching angular acceleration have the increasing trend, and the RMS are different in the cases which implies that the responses of vehicle suspension system may be affected by the traveling con-

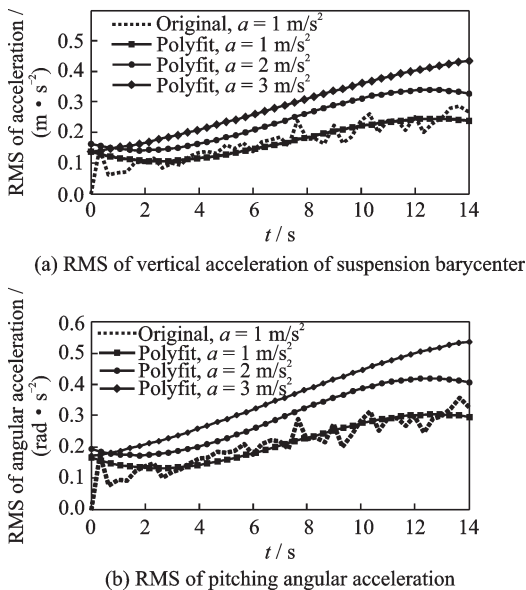
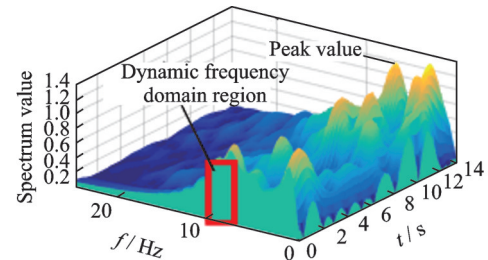


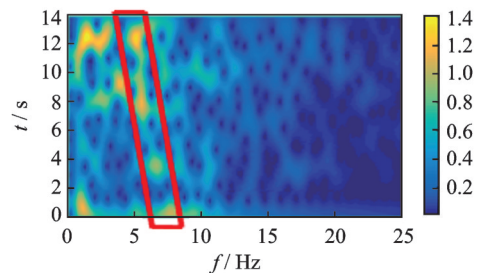
Fig.9 RMS of responses under different accelerating conditions

ditions.

The former study only gives the response analysis of suspension systems in time domain, but the analysis in frequency domain is not presented. However, the latter attracts more interest. Take the vertical acceleration response for time-frequency analysis and the time-frequency spectrum diagram is given in Fig.10. Fig.10 clearly presents the response varying tendency in both time and frequency domains. The yellow region in the red parallelogram represents the DFD of the responses. The initial central frequency is about 8 Hz and moves toward the lower frequency region continually with the increased speed. The result shows that the response of suspension in this case may not be stationary process, and the DFD has changed obviously.



(a) Dynamic frequency domain in three-dimensional diagram



(b) Tendency of frequencies corresponding to peak-values

Fig.10 Time-frequency analysis result of vertical acceleration of suspension barycenter

The frequencies corresponding to the peak values of response spectrum is bound to shift from high to low frequency because of the variable-speed traveling. That is to say, in non-stationary situation, we have to use time-frequency analysis method to study the responses of suspension systems. According to Fig.10, at the starting moment, the frequency corresponding to the peak values of response spectrum is 8 Hz, and it changes as the vehicle speeds up. However, the frequencies still belong to the sensitive

band of human's body. The results show that the concept of DFD is of great significance for the analysis of vehicle suspension response, and the suspension control with ride comfort as the goal should be based on the finite frequency domain.

4 Conclusions

The dynamic response analysis of vehicles under non-stationary random excitation condition has become the research hotspot. Based on the human's sensitive to vibration in different frequency range, some conclusions can be drawn from our study.

(1) The paper proposes a new concept named DFD analysis which would be a new innovation in non-stationary random vibration research field. It is the basement of non-stationary random vibration control for vehicles traveling in complex cases. More works should be conducted with this concept and advanced algorithms would be developed by our research team in the future.

(2) The excitations to the front and the rear wheels in time domain are derived and the digital process is acquired using PTIM. This method has more precise advantages compared with the traditional numerical methods such as Newmark and Wilson- θ .

(3) By analysing the responses of vertical acceleration at the barycenter of suspension and pitching angular acceleration of suspension in three different accelerations, 1 m/s^2 , 2 m/s^2 , 3 m/s^2 , the RMS tendency are obtained.

(4) In addition, the time-frequency spectrum diagram is obtained by using time-frequency analysis method, and the results show that the RMS increases with the increase of speed and the range of interest of DFD moves to the low frequency region, which can provide an important reference for the design and application of active suspension.

References

- [1] MAO C, JIANG Y, WANG D, et al. Modeling and simulation of non-stationary vehicle vibration signals based on Hilbert spectrum[J]. *Mechanical Systems and Signal Processing*, 2015(50/51): 56-69.
- [2] MARIA A P. A review of experimental techniques for NVH analysis on a commercial vehicle[J]. *Energy Procedia*, 2015(82): 1017-1023.
- [3] MASSIMO G. The science of vehicle dynamics: Handling, braking, and ride of road and race cars [M]. 1st ed. Dordrecht: Springer, 2014: 235-270.
- [4] JAMES M H. Characterising the in-vehicle vibration inputs to the high voltage battery of an electric vehicle[J]. *Journal of Power Sources*, 2014 (245): 510-519.
- [5] WANG C, LI W, ZHAO W, et al. Torque distribution of electric vehicle with four in-wheel motors based on road adhesion margin[J]. *Transactions of Nanjing University of Aeronautics and Astronautics*, 2019, 36 (1): 188-195.
- [6] TANG X, YANG W, HU X, et al. A novel simplified model for torsional vibration analysis of a series-parallel hybrid electric vehicle[J]. *Mechanical Systems and Signal Processing*, 2017, 85: 329-338.
- [7] ROHIT J, OLAF B, FADIL A, et al. An observational study of the effect of vibration on the caking of suspensions in oily vehicles[J]. *International Journal of Pharmaceutics*, 2016, 514(1): 308-313.
- [8] DIMITRIS S P, HANS V G, STAVROS G V. Country road and field surface profiles acquisition, modeling and synthetic realization for evaluating fatigue life of agricultural machinery[J]. *Journal of Terramechanics*, 2016(63): 1-12.
- [9] NGWANGWA H M, HEYNS P S, BREYTENBACH H G A, et al. Reconstruction of road defects and road roughness classification using artificial neural networks simulation and vehicle dynamics responses: Application to experimental data[J]. *Journal of Terramechanics*, 2014(53): 1-18.
- [10] PARKHILOVSKII I G. Investigation of the probability characteristics of the surfaces of distributed types of roads[J]. *Avtom Prom*, 1968 (8): 18-22.
- [11] DODDS C J, ROBSON J D. The description of road surface roughness[J]. *Journal of Sound and Vibration*, 1973, 31(2): 70-75.
- [12] LIN J. Identification of road surface power spectrum density based on a new cubic spline weight neural network[J]. *Energy Procedia*, 2012 (17): 534-539.
- [13] KAZEM R K, MOHAMMAD J, ALIREZA A. Investigating the effect of road roughness on automotive component[J]. *Engineering Failure Analysis*, 2014 (41): 96-107.
- [14] XIE X, WANG D, LIU D, et al. Investigation of synthetic, self-sharpening aggregates to develop skid-resistant asphalt road surfaces[J]. *Wear*, 2016 (348/349): 52-60.
- [15] AU F T K, CHENG Y. Effects of random road sur-

- face roughness and long-term deflection of prestressed concrete girder and cable-stayed bridges on impact due to moving vehicles[J]. *Computers and Structures*, 2001(79): 853-872.
- [16] SCHIEHLEN W, HU B. Spectral simulation and shock absorber identification[J]. *International Journal of Non-Linear Mechanics*, 2003(38): 161-171.
- [17] TRICOT C. A model of rough surfaces[J]. *Composite Science and Technology*, 2003(63): 1089-1096.
- [18] MARZBANRADA J, AHMADIB G. Stochastic optimal preview control of a vehicle suspension[J]. *Journal of Sound and Vibration*, 2004(275): 973-990.
- [19] ZHANG Buyun, CHEN Huaihai, WANG Ruochen, et al. New random signals generating method for multiple excitation vibration system based on white noises[J]. *Journal of Nanjing University of Aeronautics and Astronautics*, 2017, 49 (6): 839-844. (in Chinese)
- [20] NING J, LIN J, ZHANG B. Time-frequency processing of track irregularities in high-speed train[J]. *Mechanical Systems and Signal Processing*, 2016, 66/67: 339-348.
- [21] LORENZO C, MARTIN C, JANKO S, et al. Non-stationary index in vibration fatigue: Theoretical and experimental research[J]. *International Journal of Fatigue*, 2017, 104: 221-230.
- [22] SHEN J, WU L. A non-stationary random vibration analysis of vehicle-bridge coupling under road surface coherence excitation[J]. *IOP Conference Series: Earth and Environmental Science*, 2019, 376: 012027.
- [23] LEI Liangyu, ZHANG Weiping, WANG Jiangtao. Simulation and analysis on nonstationary random road[J]. *Chinese Journal of Sensors and Actuators*, 2007, 20(4): 877-880. (in Chinese)
- [24] ZHANG Lijun, ZHANG Tianxia. General nonstationary random input model of road surface with four wheels correlated[J]. *Journal of Vibration and Shock*, 2008, 27(7): 75-78. (in Chinese)
- [25] MICHAELOV G, SARKANI S, LUTES L D. Spectral characteristics of nonstationary random processes—A critical review[J]. *Structural Safety*, 1999 (21): 223-244.
- [26] MICHAELOV G, SARKANI S, LUTES L D. Spectral characteristics of nonstationary random processes—Response of a simple oscillator[J]. *Structural Safety*, 1999(21): 245-267.
- [27] MARBATO M, CONTE J P. Spectral characteristics of non-stationary random processes: Theory and applications to linear structural models[J]. *Probabilistic Engineering Mechanics*, 2008(23): 416-426.
- [28] ZHONG Wanxie. On precise time-integration method for structural dynamics[J]. *Journal of Dalian University of Technology*, 1994, 34 (2) : 131-136. (in Chinese)
- [29] MOLER C, LOAN C C. Nineteen dubious ways to compute the exponential of a matrix[J]. *SIAM Review*, 1978, 20(4): 801-836.
- [30] MOLER C, LOAN C C. Nineteen dubious ways to compute the exponential of a matrix, twenty-five year later[J]. *SIAM Review*, 2003, 45(1): 1-46.
- [31] ZHANG Lijun, ZHANG Tianxia. A study on road random inputs to a vehicle with uneven speed in time and frequency domains[J]. *Automotive Engineering*, 2005, 27(6): 710-714. (in Chinese)

Acknowledgement This work was supported by the National Natural Science Foundation of China (No. 51705205).

Author Dr. ZHANG Buyun received his B.S. degree in mechanical engineering and automation from China University of Mining and Technology (CUMT), Xuzhou, China, in 2009 and Ph.D. degree in engineering mechanics from Nanjing University of Aeronautics and Astronautics (NUAA), Nanjing, China, in 2015. Since July 2015, he has been a faculty member at the Automotive Engineering Research Institute, Jiangsu University, Zhenjiang, China. From December 2019, he is a visiting scholar at Wayne State University, Detroit, USA, researching on non-stationary vehicle dynamics, with applications to smart suspension systems in autonomous vehicles with road preview. His research interests include algorithms in vibration environment testing and control, vehicle lightweight design, structural modeling and testing, and non-stationary random analysis of vehicle dynamics.

Author contributions Dr. ZHANG Buyun designed the study, proposed the dominant concept, conducted the analysis, interpreted the results and wrote the manuscript. Dr. ZENG Falin contributed to the background of the study, the data and the simulation. Prof. TAN Chin-An polished English writing of the manuscript, and interpreted the results.

Competing interests The authors declare no competing interests.

基于时频谱的变速行驶车辆悬架系统动态共振频域特性研究

张步云¹, 曾发林¹, TAN Chin-An²

(1. 江苏大学汽车工程研究院, 镇江 212013, 中国; 2. 美国韦恩州立大学机械工程学院, 底特律 48202, 美国)

摘要: 车辆变速行驶时悬架系统的动态响应通常是非平稳随机过程, 对其进行时频分析是近年来车辆平顺性研究中的重点与热点问题。本文依据人体对不同频带的振动敏感性不同, 提出动态频域概念以开展非平稳车辆动力学评价研究, 主要包含前后轮输入数值分析与非平稳随机激励下悬架系统时频特性研究。应用精细积分法获得悬架系统的垂向加速度与俯仰角加速度, 研究不同加速度工况下的响应均方根值。结果表明, 非平稳激励下响应均方根值为时间的函数, 同时随速度增加而增大, 且垂向加速度的动态频域区间有向低频迁移的趋势, 可为复杂驾驶工况下主动悬架的设计提供重要参考依据。

关键词: 非平稳随机过程; 悬架系统; 车辆建模; 动态频域; 平顺性